Probing the Effects of Calcium on Gelsolin

Brian J. Pope, John T. Gooch, and Alan G. Weeds*

MRC Laboratory of Molecular Biology, Hills Road, Cambridge CB2 2QH, U.K.

Received September 4, 1997; Revised Manuscript Received October 16, 1997[⊗]

ABSTRACT: Gelsolin is a calcium-regulated actin severing and capping protein that binds two calcium ions and has three sites for actin; two recognize monomeric actin and one attaches to the sides of filaments. It contains six repeating sequence segments (G1−6). Here, we have analyzed the effects of calcium ions on (i) limited proteolysis of bacterially expressed human gelsolin by plasmin and (ii) dynamic light scattering and circular dichroism of gelsolin and various of its subdomains. Following cleavage of gelsolin in the absence of calcium between Lys_{150} and His_{151} (the junction between G1 and G2), the molecule does not fall apart, nor does it bind actin without added calcium. This same molecule can be reconstituted by mixing an excess of G1 with G2−6 in EGTA. The noncovalently linked form of gelsolin shows three actin binding sites in calcium and requires 3 μM calcium for 50% activation of actin binding. Measurements of light scattering and circular dichroism revealed structural changes in response to calcium for intact gelsolin and a number of its actin-binding subdomains. Many of these changes occurred at calcium concentrations below 100 nM. These results are discussed in relation to the calcium control of gelsolin function and its three-dimensional structure (Burtnick *et al.* (1997) *Cell 90*, 661−670). Nanomolar concentrations of calcium initiate the unlatching of structural constraints that maintain the inaccessibility of the actin binding sites, but actin binding occurs only after additional micromolar calcium sites in both the N-terminal and C-terminal halves of the molecule are occupied.

Gelsolin (GS)[1] was first identified as a calcium-dependent actin filament destabilizing protein present in macrophages and blood plasma (*1*−*3*). It is a member of a ubiquitous family of severing proteins that contain either six (GS, villin, adseverin) or three repeating segments (fragmin, severin) (reviewed in ref *4*). The six segments of GS (here denoted G1−6), identified on the basis of their sequence homology *(5)*, have recently been shown to contain the same basic structural fold *(6)*. GS has two binding sites for monomeric actin, a calcium-independent site in G1 (K_d = 5 pM) and a calcium-dependent site in G4 (K_d = 1.8 μM, but = 25 nM as part of the larger construct G4−6) and one site for F-actin, located in G2 (K_d = 5−7 μM) *(7*−*9)*. The minimal actin severing domain is G1−2 *(9)*, while full nucleating activity requires the two actin binding sites in G2−6 *(10)*. The former is calcium independent, while the latter requires calcium, showing that calcium regulation of all three actin-binding sites is mediated through the C-terminal half of the molecule.

Activation of GS requires calcium ions, but the mechanism is unclear and there is ambiguity in the literature about the levels of calcium required for activation. Two calcium binding sites were identified by equilibrium dialysis with a $K_d \sim 1$ μM (ref *11* and references therein). Similar experiments identified two calcium binding sites in G4−6, a high affinity site located in G5−6 ($K_d \sim 0.2$ μM) and a lower affinity site in G4−5 ($K_d \sim 2$ μM) *(8)*. Using photon correlation spectrosopy and depolarized dynamic light scattering, Patkowski et al. obtained evidence for a significant conformational change when GS binds calcium, which depends on calcium binding to G4−6 *(12, 13)*. Thus, it appears that calcium binding to G4−6 induces structural changes that allow actin to bind. Since GS binding to G-actin is cooperative *(14, 15)*, association of the first actin with the calcium-sensitive site in G4−6 facilitates further actin binding to G1, which results in trapping of calcium in the complex between actin and the G1 site *(16, 17)*. Selve and Wegner reported that ternary complex formation reached a maximal rate at 1 μM calcium *(18)*, but more recent experiments have shown that the association of GS with one actin monomer is regulated by calcium with a K_d = 25 μM *(19)*. Elsewhere, it has been reported that half-maximal activation of severing and nucleating activities occurs at ∼10 μM calcium *(20)*, and it is evident that the rate-limiting step in the severing process is the activation of GS by the binding of divalent cations to low affinity sites. Thus, it appears that while GS has high affinity calcium-binding sites associated with the C-terminal half of the molecule, which may be involved in the initial opening of the molecule, higher calcium concentrations are required to promote actin binding and full severing activity. Recent structural analysis of the inhibited form of GS (in the presence of EGTA) has provided evidence for a noncovalent interaction between the C-terminal part of G6 and G2, which renders all three actin-binding sites inaccessible *(6)*. Thus, calcium binding to G5−6 may unlatch this lock, but this action alone does not appear to be sufficient to activate the molecule.

Here we have analyzed the effects of calcium on GS and various of its subdomains, using far-UV circular dichroism (CD), dynamic light scattering (DLS), and biochemical studies of proteolytic susceptibility. Far-UV CD measurements revealed a marked calcium specific effect at nanomolar levels. Similar concentrations also resulted in molecular

* To whom correspondence should be addressed. Tel.: England 1223 402 401. Fax 1223 213 556. E-mail: agw@mrc-lmb.cam.ac.uk.

[⊗] Abstract published in *Advance ACS Abstracts*, December 1, 1997.

[1] Abbreviations: The six repeating segments of sequence in gelsolin are denoted G1−6; CD, circular dichroism; DLS, dynamic light scattering; GS, gelsolin.

S0006-2960(97)02192-2 CCC: $14.00

rearrangements in DLS experiments, but although these were initiated at the nM level, the effect was only complete with μM free calcium. Our experiments have also revealed a strong noncovalent association between G1 and G2−6, which holds the molecule in the closed state in the absence of calcium. The results show that molecular rearrangements occur within individual domains, which we have modeled in terms of the three-dimensional structure *(6)*. We have also identified a third calcium binding site in G1−3 ($K_d \leq 0.2$ μM). Binding of submicromolar calcium concentrations causes condensation of segments G4−6. This in turn leads to an increase in radius of the GS molecule as the C-terminal α-helix of G6 releases its clamping effect on G2. Further calcium binding in the micromolar range releases the "latch" between G1 and G3, which opens the molecule and makes the actin binding sites in G1 and G2 accessible.

MATERIALS AND METHODS

Construction and Expression of Human Gelsolin Segments. Plasma G1−5 (defined as amino acid residues Ala_1-Lys_{634}) was prepared by modification of the cDNA clones for human plasma GS and G2−5 that had been previously engineered into the pMW172 expression vector *(21)*. These were each digested with MscI and HindIII and the MscI-HindIII G2−5 insert ligated into the MscI-HindIII vector portion of the GS. This yields a construct carrying an MGSIEGR leader sequence (for which the Met is not processed in *E. coli*) with a flush C-terminal.

E. coli cell cultures of the various constructs (1 L) were centrifuged and the cell pellets frozen. Either soluble fractions or inclusion bodies, as appropriate, were prepared *(9)*. G1−5 was isolated from inclusion bodies and purified in 10 mM Tris−HCl pH 8.0, 0.2 mM EGTA, 1 mM NaN_3 (buffer A) initially by chromatography on a 10 × 2.5 cm DEAE−cellulose column (Whatman DE52). Although G1−5 does not bind, most of the contaminants are retarded. The pH of the flow through was lowered to ∼6.3 with 1 M succinic acid pH 6.0, and the protein was loaded onto a (carboxymethyl)cellulose column (Whatman CM52) equilibrated in 10 mM succinic acid pH 6.0, 0.2 mM EGTA, and 1 mM NaN_3. Elution was by gradient to 0.25 M NaCl.

GS was purified using a modification of the method of ref *22*. GS expressed in the soluble fraction of *E. coli* was loaded directly onto a 10 × 2.5 cm column of Sigma Cibacrom blue 3G-A in buffer A and eluted with the same buffer containing 1.0 mM ATP. This gives pure GS after removal of the ATP, either by prolonged dialysis or gel filtration on a Pharmacia P10 column. An alternative method, used for larger volumes, was to repeat the Cibacrom blue chromatography, using Ca^{2+} to displace bound ATP from GS *(23)*: the column was prewashed with buffer A containing 0.5 M NaCl to remove contaminants before regeneration in buffer A containing 1.0 mM Ca^{2+} in place of the EGTA. The GS was also treated with 1 mM Ca^{2+} before reapplying to the column, which was then washed in buffer A containing 1 mM Ca^{2+} to remove all traces of the ATP. Gelsolin was eluted with buffer A containing 1 mM Ca^{2+} and 0.5 M NaCl. G4−6, G2−6, and plasma G1were all prepared as described previously *(24)*.

Purified proteins were either dialysed into 2.5 or 10 mM Tris−HCl pH 8.0, 0.2 mM EGTA, 50 mM NaCl, or changed into these buffers on Pharmacia P10 desalting columns. Where necessary, they were concentrated on Amicon centricon units, and all samples were filtered through a 0.1 μm membrane. Protein concentrations were calculated from absorbance measurements at 280 nm, based on the tyrosine and tryptophan content of each construct *(25)*. Values for $A_{280} = 1.0$ cm^{-1} were G4−6 = 15.3 μM, G2−6 = 10.7 μM, G1 = 48.9 μM, G1−5 = 12.1 μM, and GS = 8.9 μM.

Proteolysis. Proteins in 10 mM Tris−HCl pH 8.0, 50 mM NaCl, and 1 mM NaN_3 were digested at 21 °C with 1:10 w/w human plasmin (Sigma) for between 30 min and 4 h in Ca^{2+} or overnight in EGTA. Digestion was terminated with a 100-fold molar excess of N_α-*p*-tosyl-L-lysine chloromethyl ketone using a 10 mg/mL stock in 1 mM HCl.

Antibody Staining for Gelsolin. Monoclonal anti-GS (Sigma G-4896) was used to identify C-terminal fragments of GS in the proteolytic digests. We have characterized this antibody using human GS constructs previously generated in this laboratory *(8)*. It recognizes only constructs containing G5. However, because we cannot prepare G6 in isolation, we cannot exclude the possibility of some binding to this segment also.

Chromatography. Gel filtration was performed on a 30 × 1.0 cm Sephacryl S-200 column in 10 mM Tris−HCl pH 8.0, 50 mM NaCl, 1 mM NaN_3 with either 0.2 mM EGTA or 0.1−1 mM Ca^{2+}, collecting 0.6 mL fractions. Plasmin digests of GS were analyzed by ion-exchange chromatography on a 10 × 2.5 cm DEAE column (Whatman DE52) in buffer A ± Ca^{2+}. Cibacrom blue affinity columns were used both to purify GS and to assay individual domains for the ATP binding site.

Actin Binding Assays. Rabbit skeletal muscle actin was prepared and chemically modified as described previously *(9)*. Its concentration was determined using an extinction coefficient $A_{290} = 1.0$ cm^{-1} = 35.9 μM. Sedimentation assays were performed following a 10 min incubation at 21 °C of 3 μM F-actin with 3 μM G1−5 or using 10 μM actin for the plasmin digested GS *(8)*. NBD-actin (actin reacted with *N*-ethylmaleimide on Cys 374 and then on Lys 373 with 7-chloro-4-nitrobenzeno-2-oxa-1,3-diazole) was used to measure binding to monomeric actin in 10 mM Tris−HCl pH 8.0, 0.2 mM ATP, 0.2 mM dithiothreitol, 1 mM NaN_3, and either 0.2 mM $CaCl_2$ or 0.2 mM $MgCl_2$ + 0.2 mM EGTA *(9)*. Nucleating activity was assayed using PI-actin *(26)*. G-actin (6 μM) containing 14% PI-actin was treated with 0.2 mM EGTA and 0.2 mM $MgCl_2$ for 90 s before further addition so that assays were all performed on Mg^{2+}-actin. After preincubation, G1−5 and then 1 mM Mg^{2+} with 100 mM NaCl were added to initiate polymerization. To test for calcium dependence, 0.2 mM Ca^{2+} was added with the G1−5.

Dynamic Light Scattering. DLS was performed in a DynaPro-801 dynamic light-scattering instrument (Protein Solutions Ltd, The Hillside Centre, Upper Green Street, High Wycombe, Buckinghamshire HP11 2RB, U.K.). Protein solutions at 1−2 mg/mL were analyzed for translational diffusion coefficient (D_T) which, under the assumption of Brownian motion, was then translated using the Stokes−Einstein equation to the hydrodynamic radius (R_H) from which an estimate of the apparent M_r was made assuming the proteins are globular and of standard density. Monodisperse data point sets were analyzed using a monomodal curve fit analysis and 10 such points averaged for each

determination. Solutions exhibiting any proportion of mixed populations were processed to fit a bimodal size distribution, but molecular weights estimated in this way were not as accurate.

Circular Dichroism. Far-UV CD measurements were made on a Jobin-Yvon Dichrograph CD6 using 300 μL of protein in the concentration range of 0.2−0.6 mg/mL in 2.5 mM Tris−HCl pH 8.0, 0.1 mM EGTA, 1 mM $MgCl_2$, and 50 mM NaCl at 20 °C in a 1 mm path-length cell at 20 °C. To change the Ca^{2+} concentration, 1−3 μL additions of 10−100 mM $CaCl_2$ were added and mixed in the cuvette. Data were collected at 0.5 nm intervals with two data points per minute. Five such runs were averaged, calculated net of buffer, and factor 3 smoothed. The percent α-helix was estimated from complete data sets in the CONTIN program *(27)*.

Calcium Concentrations and Calcium Binding. Free calcium concentrations were calculated at equilibrium in the various Ca^{2+}, Mg^{2+}, EGTA, and (where appropriate) ATP buffers using the EQCAL program of Biosoft, Hills Road, Cambridge, CB2 1JP, U.K. Calcium binding was measured by equilibrium dialysis as previously described *(8)*.

RESULTS

G1−5 Purification and Actin Binding. We have previously shown that G2−6 and G1−3 bind two actin monomers, the former cooperatively in a calcium-dependent manner, while the latter is calcium independent. G2−6 has a nucleating activity similar to GS but does not sever filaments: G1−3 severs but does not nucleate *(10)*. G1−5 expressed in high levels equivalent to those reported for GS and G1 *(21)* and was readily purified to homogeneity as described in the Material and Methods. Like G1−3, it severs filaments efficiently in a calcium-independent manner (data not shown). Measuring the effects of G1−5 on the polymerization rate of 6 μM G-actin gave nucleating activities 17% and 14% that of GS in calcium and EGTA, respectively. Thus, compared to G1−3, which does not nucleate polymerization *(10)*, G1−5 has a weak nucleating activity. These results confirm the importance of G6 for nucleation as previously reported *(28)*.

Gelsolin Purification and ATP Binding. Bacterially expressed GS binds to Cibacrom blue resin in EGTA and is eluted in pure form with ATP *(29)*. This correlates with the finding that GS binds ATP in the absence of calcium with a K_d of 2.4 μM *(23)*. It provides a single-step purification of the protein from bacterial extracts. G2−6 and G1−5 also bound to Cibacrom blue resin, but neither eluted with ATP, which suggests that the ATP binding site in GS requires that the protein be in the closed EGTA state and involves the participation of G1.

Plasmin Digestion of Gelsolin Yields a Noncovalently Linked Product That Does Not Fall Apart in the Absence of Calcium. Plasmin digestion for 30 min at 1:25 w/w ratios produced a single cleavage in GS. Even after overnight exposure to plasmin in Ca^{2+} or EGTA at 1:10 w/w there was no further digestion. We identified the cleavage site by amino-terminal sequencing to be between Lys_{150} and His_{151} in plasma GS on the G1−G2 boundary, in agreement with ref *30*. This serves as a useful method to prepare G2−6 directly from GS. The two should be well separated on a DEAE column based on the predicted net charges at pH 8.0 (plasma-G1 = 0; cytoplasmic-G1 = −2 and G2−6 = −12). However, the elution profile showed a single peak at 130 mM salt in the position expected for intact cytoplasmic GS (Figure 1). Likewise, the digest ran as a single unit on sizing columns clearly indicating that although cleaved, as analyzed by SDS PAGE, the fragments were maintained as an intact unit. The two fragments separated on addition of calcium (Figure 1), where cytoplasmic G1 elutes at 8 mM and G2−6 at 75 mM salt. To test the specificity of calcium, 1 mM Mg^{2+} was added and the digest rechromatographed on an S200 column. There was no release of G1 from G2−6 in the absence of calcium, but complete disassociation occurred at 10 μM free calcium.

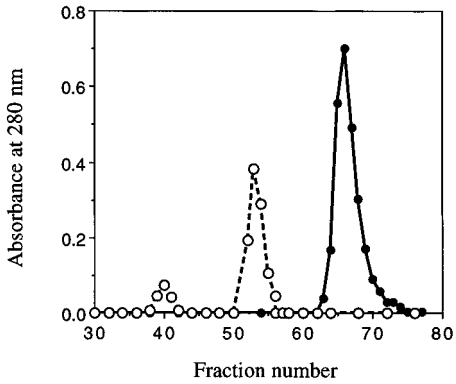

FIGURE 1: DEAE cellulose chromatography of cytoplasmic GS cleaved at the G1/G2−6 boundary with plasmin. Columns run in 10 mM Tris pH 8.0, with 0.2 mM EGTA (closed circles) or 0.1 mM Ca^{2+} (open circles). The peak eluting at tube 40 is free G1 (8 mM salt), peak 2 around tube 55 is free G2−6 (75 mM salt), and peak 3 at tube 66 is G1 complexed with G2−6 (130 mM salt).

Acidification of the digested protein with 50 mM succinate to pH 6.0 also dissociated the G1 and G2−6. This is consistent with the loss of calcium requirement for filament severing and nucleation of GS on acidification, reported elsewhere *(20)*.

The digested GS was assayed for F-actin binding by cosedimentation. In EGTA it remained in the supernatant while most of the actin pelleted, but in calcium at a molar ratio of 0.5/actin, the G2−6 was mainly associated with the actin pellet, while the G1 was in the supernatant with some additional actin. Thus, the digested protein shows calcium-sensitive actin binding with G1 releasing actin subunits into the supernatant and residual pelleted F-actin binding the G2−6 via the F-actin binding domain in G2.

Reconstitution of "Gelsolin" from G1 and G2−6. Plasma G1 and G2−6 were expressed separately and purified from *E. coli*. The two were mixed together in 10 mM Tris−HCl pH 8.0, 0.2 mM EGTA, 50 mM NaCl, and 1 mM NaN_3 at ratios of between 1:1 and 15:1 G1:G2−6 and left at 4 °C overnight. Fractionation on S200 Sephacryl showed two peaks, the first, eluting at the position expected for intact GS, contained both G1 and G2−6 while the second contained only G1. Densitometry of nondenaturing gels of samples from the first peak showed an equimolar ratio of G1 and G2−6 = 1.02 ± 0.18, (n = 9). Similar recombination experiments using plasma-G1:G2−6 (2:1 mol/mol) were analyzed using nondenaturing gels (Figure 2). G2−6 and plasma-GS carry the same net charge of −12, but the G2−6 (M_r 67.2 kDa) runs faster than the GS (M_r 83.6 kDa). From Figure 2 it can be seen that plasma G1 associates with G2−6 to give a complex of similar mobility to plasma GS. Using

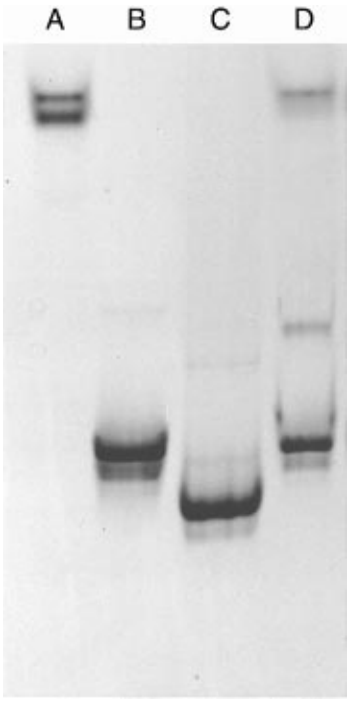

FIGURE 2: Nondenaturing PAGE from G1/G2−6 reconstitution/recombination experiments showing (A) plasma-G1 (lower band = monomer, upper = dimer), (B) plasma-GS, (C) G2−6, and (D) a complex from plasma-G1 mixed with G2−6 in the presence of 0.2 mM EGTA at a molar ratio of 2:1.

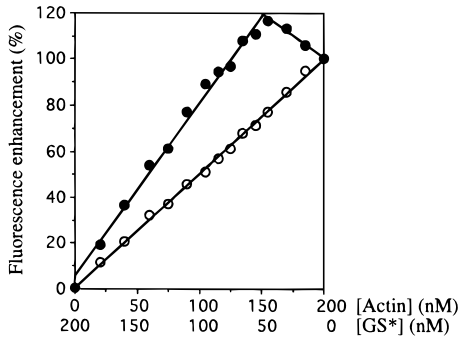

FIGURE 3: Fluorescence titrations at constant total protein concentration (200 nM) with continuous variation of both NBD−actin and reconstituted GS (GS*). Analyses were carried out in 0.2 mM $CaCl_2$ (solid symbols) or 0.2 mM $MgCl_2$ + 0.2 mM EGTA (open symbols) at pH 8.0.

different ratios of G1 to G2−6 showed that complex formation was maximal when G1 and G2−6 were mixed at a 2:1 ratio. It should be noted that G1 has a tendency to aggregate and runs as a doublet of monomer and dimer on nondenaturing gels, but only the monomer form reassociates with G2−6 to reconstitute this noncovalently linked "GS". Similar experiments showed no association between G1 and either G4−6, G2−3, or G2−5, which confirms the specificity of the noncovalent association of G1 with G2−6.

The reconstituted GS was also tested for actin binding using the fluorescence enhancement of NBD-actin, with continuous variation of both components as described previously *(10)*. Figure 3 shows that there is no enhancement of fluorescence in EGTA, but in calcium the actin fluorescence is increased to a maximum at 151 nM actin and 49 nM GS, i.e., a molar ratio of three actins per GS. Thus, as expected, addition of calcium causes dissociation of the reconstituted GS into G1 and G2−6, the former binding a single actin monomer and the latter two. The calcium

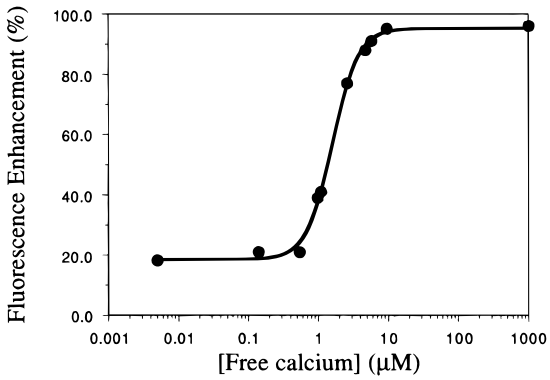

FIGURE 4: Fluorescence enhancement on mixing 0.5 μM reconstituted GS with 1.5 μM G-actin at pH 7.1 in the presence of 0.196 mM EGTA and various calcium concentrations to give the free calcium concentrations shown. Non-linear least-squares fitting suggested a K_d of 3 μM and cooperative binding with a Hill coefficient of 2.3.

dependence of fluorescence enhancement is shown in Figure 4: 50% activation occurred at 3 μM calcium. On the basis of these experiments, it is clear that G1 and G2−6 reassociate in the absence of calcium to give a product in which, like intact GS, all the actin binding sites are inaccessible.

Further Digestion by Plasmin. A second plasmin cleavage site has been identified in GS lacking the disulfide bond between Cys_{188} and Cys_{201} in G2 *(30)*. The fact that we see only a single cleavage suggests that our GS is in the oxidized state, like native plasma GS. To test this, the bacterially expressed GS was unfolded with 8 M urea and treated with 1 mM DTT before refolding by dialysis against 10 mM Tris−HCl pH 8.0, 0.2 mM EGTA, and 1 mM NaN_3. Plasmin digestion now showed a second cleavage site, between Arg_{228} and Ala_{229}, similar to that reported elsewhere *(30)*. The reduced form of GS with the second plasmin cut did not hold together in EGTA, giving two fragments on either gel filtration or native gel electrophoresis. These results demonstrate that in contrast to the the methods used in Boston *(30)*, our bacterially expressed GS preparation is isolated in the native form.

G2−3, G1−3, and G1−5 were also treated with plasmin to explore their susceptibility to proteolysis. G1−5 was degraded more rapidly than GS or the other constructs, giving significant cleavage to G2−5 within 1−2 min in calcium but no significant further change in the pattern of digestion over 4 h. G1−5 was even more susceptible to proteolysis in EGTA (Figure 5). Using the Sigma monoclonal antibody to GS, for which we mapped the epitope to G5, we found that all of the major degradation products contained G5, showing that cleavage occurred exclusively at the N-terminal end. N-Terminal analysis identified Ala_{229} (removing two-thirds of G2) and Asn_{368} (two-thirds of G3) as the main cleavage sites. G1−3 digested to G1 and G2−3 in calcium but, like G1−5, was more extensively cleaved in EGTA. G2−3 was stable to plasmin digestion in calcium but proteolyzed in EGTA. Thus, the presence of calcium protects sites in the G2−3 domain of all these expressed constructs.

Dynamic Light Scattering. It is clear from the differences in proteolytic susceptibility that the structure of GS is affected by calcium, not just at the contact site between G6 and G2 *(6)*, but also in G2−3. Large changes in the apparent M_r were observed for all constructs on binding calcium (Table

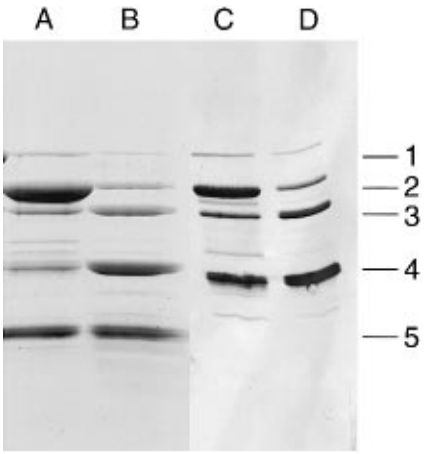

FIGURE 5: Polyacrylamide gel electrophoresis of plasmin digests of G1−5: (A) 3 h digestion in calcium; (B) 3 h digestion in EGTA. The major bands are as follows: 1 = G1−5, 2 = G2−5 (His_{151} N-terminus), 3 = G3−5 (Ala_{229} N-terminus), 4 = G4−5 (Asn_{368} N-terminus), 5 = G1. C and D are immunoblots of A and B using the monoclonal antibody specific for G5.

Table 1: Summary of the Effects of Ca^{2+} on the Changes in Hydrodynamic Radii (R_H) and Apparent M_r As Determined by Dynamic Light Scattering[a]

construct	R_H DLS (%)	apparent M_r DLS (%)	% α-helix CD	backbone CD
GS	+11	+28	−6.7	less structured
G2−6	+5	+13	−6.5	less structured
G1−3	−5	−11	no change	less structured
G1−5	−8	−16	+10.3	more structured
G4−6	−7	−15	+13.4	more structured

[a] % α-helix is from the mean residue ellipticity at 222 nm (peak of α-helical activity) and general backbone structure by CD. Note that the changes in CD responses occurred at calcium concentrations in the low nanomolar range, but light scattering changes needed close to micromolar calcium for completion.

1). GS gave a monomodal distribution in EGTA with an estimated M_r of 82 800, which compares well with the true M_r of 83 600. The polydispersity measurements were below detection limits, which coupled with an average base line value of 0.999 and sum of squares error of 0.167, indicated a fully monodisperse solution. Addition of calcium to 1 mM increased the radius from 3.93 to 4.36 nm and the estimated M_r to 106 100 in good agreement with the M_r of 110 000 in calcium estimated from S200 column chromatography *(15)*. Calcium did not affect the polydispersity, indicating that the changes in apparent M_r were due solely to changes on the radius of the molecule and not self-association. The change in apparent M_r was monitored as a function of calcium concentration starting from the EGTA state, with additions of calcium to a maximum of 10 μM free calcium and then reversing the process by adding EGTA (Figure 6). These effects were fully reversible. A 50% change in apparent M_r occurred at 30 nM free calcium, and the effect was maximal at ~1 μM. G2−6, like GS, also demonstrated a similar increase in radius, translating to a higher apparent M_r in calcium.

By contrast, similar experiments using G4−6, G1−5, and G1−3 gave a reduction in apparent M_r when calcium bound. Thus, G4−6 gave a radius in EGTA of 3.53 nm, equivalent to an M_r of 64 300, which changed with calcium to a smaller radius of 3.30 nm (M_r = 55 000). The corresponding reductions in apparent M_r for G1−5 and G1−3 were 17% and 12.5%, respectively. In all cases, these effects were shown to be calcium specific (i.e., no differences ± 1 mM $MgCl_2$ using 10−1000 μM free calcium).

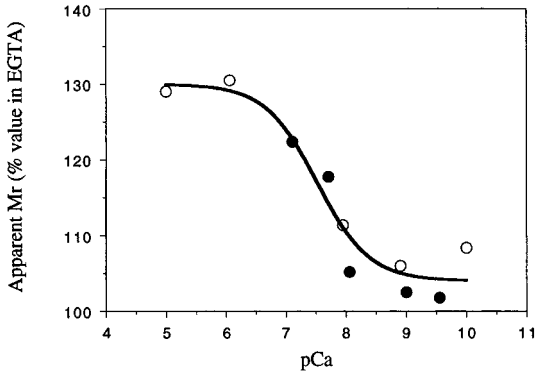

FIGURE 6: Dynamic light scattering measurements on plasma GS showing the variation of apparent M_r with pCa. Open circles are measurements starting in EGTA with additions of calcium, while closed circles show the reverse process, adding EGTA. The calcium concentration for 50% change = 30 nM.

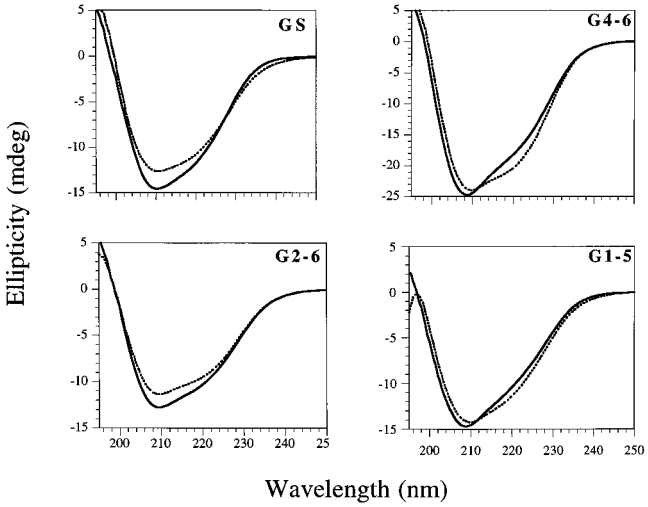

FIGURE 7: CD profiles for 2.6 μM GS, 8.2 μM G4−6, 2.8 μM G2−6, and 3.5 μM G1−5 assayed in the presence of 0.2 mM EGTA (solid lines) or 10 μM Ca^{2+} (dotted lines).

CD Measurements. Circular dichroism was used to test whether the structural changes seen by DLS might reflect any underlying changes in secondary structure. Samples were assayed in 2.5 mM Tris−HCl pH 8.0, 0.1 mM EGTA, and 50 mM NaCl and then reanalyzed following the addition of magnesium or calcium to the samples. The inclusion of 1 mM $MgCl_2$ on its own resulted in a small shift in the profile for G1−3 to one of less secondary structure (α-helix and β-strands), but no effects were seen with any of the other GS constructs.

Similar changes were seen in the CD spectra for both GS and G2−6 during the switch to calcium, indicating a shift to a more random structure (Figure 7). CONTIN program analysis *(27)* indicated a mix of ~18% α-helix, 37% β-sheet, and 44% random structure in EGTA, changing to one containing 5% more random structure in calcium. These values compare well with those of ref *31*, who calculated ~14% α-helix, 45% β-sheet, and 40% random structure for GS in the EGTA.

The profiles for G4−6 and G1−5 were similar to each other but showed the opposite effect to those for GS and G2−6 (Figure 7). Addition of calcium resulted in a major

shift at ~222 nm, a point of peak activity for α-helix, i.e., calcium binding increases the extent of α-helix. On the basis of the estimates of free calcium concentration, the spectral changes for GS, G1−5, and G2−6 at ~ 6 nM free calcium were 90% of those at 10 μM, and no further changes were detected at 1 mM calcium. To confirm that these effects were reversible, EGTA was added back to the samples in the cuvettes. Little or no reversal in CD signals was seen for any of the constructs until the calcium concentration had been reduced to sub-nM levels. Similar results were obtained for the bacterially expressed GS and the reduced GS, but there was no effect of calcium on the CD spectrum of G1 and little effect on G1−3.

DISCUSSION

Proteolytic Susceptibility. The most interesting finding in this work is that GS cleaved with plasmin at the G1/G2 boundary between Lys_{150} and His_{151} retains its structural integrity and the inaccessibility of its actin-binding sites in the absence of calcium, but on addition of calcium the G1 domain binds G-actin and G2−6 binds filaments. We also demonstrate that G1 and G2−6 associate in the absence of calcium to give a noncovalent complex that behaves like native GS in not binding actin. Three actin binding sites were detected when calcium was added, as expected since G2−6 binds two actins and G1 binds one. Half-maximal actin binding occurred at 3 μM calcium at pH 8.0 (Figure 4), and non-linear least-squares fitting suggested cooperative binding, as has previously been demonstrated for both GS and G2−6 *(10)*.

The cleavage pattern seen with our bacterially expressed GS is distinct from that reported elsewhere *(30)*. When we treated our GS with DTT to reduce the disulfide bond between Cys_{188} and Cys_{201}, plasmin gave a second cleavage between Arg_{228} and Ala_{229}. This suggests that our bacterially expressed GS is like native plasma GS in containing the disulfide bond *(30)*. Cleavage at this second position causes the digested GS to fall apart in EGTA. These results demonstrate the importance of the disulfide bond in stabilizing the structure of plasma GS. Moreover, the finding that our GS has the same proteolytic susceptibility as the plasma form explains our earlier findings that there were no significant differences in actin-binding activities of this GS and native human plasma GS *(10)*. This contrasts with the recent report showing weaker severing and nucleating activities of the bacterially expressed form lacking the disulfide *(32)*.

These results can now be considered in the light of the three-dimensional structure of GS *(6)*. On the basis of this structure, the plasmin-susceptible bond is located within G2, in a region between the N-terminal β-strand that links to G1 and the central β-sheet of G2. (Burtnick defines the domain boundaries slightly differently on the basis of the structure than those proposed earlier from the sequence repeats.) This cleavage site does not appear to be in a position to contact directly either G1 or G3 so the fact that the protein does not fall apart must depend on other interactions holding G1 in place. Burtnick has reported that G1 and G3 form an intimate contact through a continuous β-sheet, while G2 is relatively isolated from both G1 and G3 (shown schematically in Figure 8). This contact provides structural stabilization within G1−3 and probably accounts for the observation

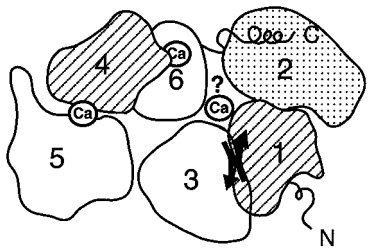

FIGURE 8: Schematic representation of the structure of GS in the EGTA form *(6)*, with G-actin binding sites on G1 and G4 (hatched) and the F-actin binding on G2 (shaded). The C-terminal α-helix from G6 interacts with G2, and the potential anti-parallel β-strand "latch" between G1 and G3 are shown as arrows. Calcium binding sites are shown between G4 and G5 and within G6 with a third site in G1−3.

that G1 and G2−6 form a noncovalent complex in the absence of calcium. Since the cleaved GS falls apart in calcium, either this contact is not maintained under these conditions or other features of the GS structure in EGTA are essential for its stability. One important feature is the noncovalent interaction between the C-terminal helix of G6 (residues 745−754) and the long helix of G2 *(6)*. This contact closes the molecule to give a globular shape with G1−3 and G4−6 related by a rotation of 180°, which places the potential actin monomer binding sites in an antiparallel orientation (Figure 8). The presence of this interaction between G6 and G2 explains earlier experiments showing that calcium control of severing activity is lost on removal of the C-terminal 23 residues of GS *(28)*.

The disulfide bond in G2 is located between the C and D strands of the β sheet that form part of the central core, parallel to the long helix. Loss of this disulfide results in additional plasmin susceptibility at Arg_{228}/Ala_{229}, i.e., between the C-terminal end of the long helix and strand E of the beta sheet, both of which appear to be close to the binding site for the C-terminal helix of G6. Since following this second cleavage the molecule does not hold together in EGTA, this suggests that the G6 helix is no longer held in place and the G1:G3 contact is consequently broken. The structural model shows that G3 is located in a postion that would prevent actin reaching the G1 binding site *(6)*. Our observations suggest that releasing the connection between G6 and G2 disrupts the G1−G3 "latch", thereby making the G1 binding site accessible.

Plasmin digestion of G1−5 showed rapid cleavage between Lys_{150} and His_{151} in both calcium and EGTA. Digestion was more rapid for G1−5 than intact GS, suggesting that the protease-sensitive site is more accessible in the absence of the G6 link. Further degradation occurred particularly in the absence of calcium, initially between Arg_{228} and Ala_{229}, then between Lys_{367} and Asn_{368} near the C-terminus of G3. These results suggest that binding the G6 helix to its site in G2 makes the cleavage site between Arg_{228} and Ala_{229} inaccessible to plasmin. The difference in proteolytic susceptibility of both G1−5 and G1−3 ± calcium supports the evidence for calcium binding to G2−3 because G1 does not bind calcium *(17)*.

Dynamic Light Scattering. Calcium increased the hydrodynamic radius of GS and G2−6, as previously reported for GS elsewhere *(12)*. The results are consistent with an opening of the molecule due to release of the G6 terminal helix from the core of G2. Half-maximal effect for GS occurred at ~30 nM calcium, a similar order of magnitude

to the calcium binding affinity of G5−6 ($K_d \sim 0.2$ μM) *(8)*. Calcium binding also affected the hydrodynamic radii of G1−5 and G4−6, but in these cases there was a reduction in apparent M_r. The results for G4−6 confirm those reported earlier *(13)*. It should be noted that the structural changes in GS occurred at a much lower calcium concentration than that needed for actin binding by reconstituted GS (50% activation at 3 μM calcium, see above). This suggests that while low calcium concentrations may promote the structural changes that unlatch the closed structure of GS, other calcium binding sites must be occupied for actin binding to occur. These could include the site in G4−5 *(8)* and possibly also that in G1−3 identified earlier *(10)*. We have repeated the equilibrium dialysis measurements for calcium binding to G1−3 and obtained saturation at ∼1.4 calcium bound per G1−3 with a $K_d \leq 0.2$ μM (data not shown). Selden et al. have also reported calcium-induced conformational changes in G1−3 related to its severing activity *(33)*.

Circular Dichroism. Changes in CD spectra were observed that mirrored the patterns seen by dynamic light scattering. Thus, the effects of calcium on GS and G2−6 were similar but opposite to those for G1−5 and G4−6. These changes occurred at very low calcium concentrations (∼10 nM). Earlier CD measurements were made either in the absence of Mg^{2+} in the near-UV with 5 mM Ca^{2+} *(34)* or in the far-UV with 100 μM Ca^{2+} *(35)*. Our results are in general agreement with these, i.e., calcium reduces the extent of secondary structure in GS. Because the structural folds of the individual domains are so similar *(6)* and not all domains bind calcium, it seems unlikely that calcium will induce large changes of secondary structure within the individual domains: rather it is the interaction between domains that is likely to be modulated by calcium ions.

While CD monitors changes in secondary structure, light scattering detects changes in the diffusional properties arising from overall shape, i.e., global arrangement of domains within GS. These responses occurred at calcium concentrations in the low nanomolar range, but the light scattering changes needed close to micromolar calcium for completion. Calcium binding sites with K_d values in the low nanomolar range have not been reported for GS, but in the case of villin, a high-affinity nonexchangeable calcium site was identified in the core domain *(36)*. (We tested for high affinity sites by denaturing GS with guanidine hydrochloride in the presence of EGTA and refolding in the presence of Ca^{45} but were unable to find any (AGW unpublished)). Thus, the only calcium binding sites to which these structural changes can at present be related are those in G5−6 ($K_d \sim 200$ nM) *(8)* and G1−3.

Model for Calcium Activation of GS. Assuming that activation of GS occurs initially by calcium binding to G6, our results suggest that this causes a condensation of G4−6 and opens the GS molecule to give a higher apparent M_r (Table 1) by releasing the link between the C-terminus of G6 and G2. This loss of constraint on G2 weakens the noncovalent bond between G1 and G3, thereby making accessible the actin binding sites required for severing (G2 and G1) and nucleation (G4−6 and G2). It is important to note that in G1−5, where this link does not exist, the actin binding sites are accessible to actin ± calcium as they are also when only the last 23 residues to GS have been removed *(28)*. Nevertheless, higher calcium concentrations are required to promote actin binding than to induce these structural changes. Our finding that reduction of the disulfide in G2 results in additional plasmin susceptibility and dissociation of the digested protein in EGTA emphasizes the importance of the stability of the structural core of G2 in holding the G6 terminal helix in place and maintaining the G1:G3 contact.

ACKNOWLEDGMENT

We are greatly indebted to Dr. Leslie Burtnick for publication of a 2D map of the crystal structure of the EGTA form of horse GS on the internet http://www.science.ubc.ca/departments/chem/brochure/burtnick.html and for sending us a preprint of his manuscript prior to publication. We express sincere thanks to Dr. Lawrence Tisi of Cambridge University Biochemistry department for help with the CONTIN calculations and to Dr Motofumi Hiyoshi for work in the preparation of the G2−5 clone.

REFERENCES

1. Chaponnier, C., Borgia, R., Rungger-Brändle, E., Weil, R., and Gabbiani, G. (1979) *Experientia 35*, 1039−41.
2. Yin, H. L., and Stossel, T. P. (1979) *Nature 281*, 583−586.
3. Harris, H., Bamburg, J., and Weeds, A. (1980) *FEBS Lett. 121*, 175−177.
4. Weeds, A., and Maciver, S. (1993) *Curr. Opin. Cell Biol. 5*, 63−69.
5. Way, M., and Weeds, A. G. (1988) *J. Mol. Biol. 203*, 1127−1133.
6. Burtnick, L. D., Koepf, E. K., Grimes, J., Jones, E., Stuart, D., McLaughlin, P., and Robinson, R. (1997) *Cell 90*, 661−670.
7. Bryan, J. (1988) *J. Cell Biol. 106*, 1553−1562.
8. Pope, B., Maciver, S., and Weeds, A. G. (1995) *Biochemistry 34*, 1583−1588.
9. Way, M., Pope, B., and Weeds, A. G. (1992) *J. Cell Biol. 119*, 835−842.
10. Way, M., Gooch, J., Pope, B., and Weeds, A. G. (1989) *J. Cell Biol. 109*, 593−605.
11. Weeds, A. G., Gooch, J., Pope, B. J., and Harris, H. E. (1986) *Eur. J. Biochem. 161*, 69−76.
12. Patkowski, A., Seils, J., Hinssen, H., and Dorfmuller, T. (1990) *Biopolymers 30*, 427−435.
13. Hellweg, T., Hinssen, H., and Eimer, W. (1993) *Biophys. J. 65*, 799−805.
14. Janmey, P. A. and Stossel, T. P. (1986) *J. Muscle Res. Cell Motility 7*, 446−454.
15. Weeds, A. G., Harris, H., Gratzer, W. B., and Gooch, J. (1986) *Eur. J. Biochem. 161*, 77−84.
16. Bryan, J., and Kurth, M. C. (1984) *J. Biol. Chem. 259*, 7480−7487.
17. McLaughlin, P. J., Gooch, J. T., Mannherz, H. G., and Weeds, A. G. (1993) *Nature 364*, 685−692.
18. Selve, N., and Wegner, A. (1987) *Eur. J. Biochem. 161*, 111−115.
19. Ditsch, A., and Wegner, A. (1995) *Eur. J. Biochem. 229*, 512−516.
20. Lamb, J. A., Allen, P. G., Tuan, B. Y., and Janmey, P. A. (1993) *J. Biol. Chem. 268*, 8999−9004.
21. Way, M., Pope, B., Gooch, J., Hawkins, M., and Weeds, A. G. (1990) *EMBO J. 9*, 4103−4109.
22. Yamamoto, H., Terabayashi, M., Egawa, T., Hayashi, E., Nakamura, H., and Kishimoto, S. (1989) *J. Biochem. 105*, 799−802.
23. Kambe, H., Ito, H., Kimura, Y., Okochi, T., Yamamoto, H., Hashimoto, T., and Tagawa, K. (1992) *J. Biochem. 111*, 722−725.
24. Pope, B., Way, M., and Weeds, A. G. (1991) *FEBS Lett. 280*, 70−74.

25. Gill, S. C., and von Hippel, P. H. (1989) *Anal. Biochem 182*, 319−326.
26. Harris, H. E., and Weeds, A. G. (1983) *Biochemistry 22*, 2728−2741.
27. Provencher, S. W. (1982) *Comput. Phys. Commun. 27*, 229−242.
28. Kwiatkowski, D. J., Janmey, P. A., and Yin, H. L. (1989) *J. Cell Biol 108*, 1717−1726.
29. Yamamoto, H., Ito, H., Nakamura, H., Hayashi, E., Kishimoto, S., Hashimoto, T., and Tagawa, K. (1990) *J. Biochem. 108*, 505−506.
30. Wen, D., Corina, K., Chow, E. P., Miller, S., Janmey, P. A., and Pepinsky, R. B. (1996) *Biochemistry 35*, 9700−9709.
31. Doi, Y., Kim, F., and Kido, S. (1990) *Biochemistry 29*, 1392−1397.
32. Allen, P. (1997) *FEBS Lett. 401*, 89−94.
33. Selden, L. A., Hurwitz, C., Kinosian, H. J., Estes, J. E., and Gershman, L. C. (1997) *Biophys. J. 72*, Th221−Th221.
34. Rouayrenc, J. F., Fattoum, A., Mejean, C., and Kassab, R. (1986) *Biochemistry 25*, 3859−3867.
35. Kwiatkowski, D. J., Janmey, P. A., Mole, J. E., and Yin, H. L. (1985) *J. Biol. Chem. 260*, 15232−15238.
36. Hesterberg, L. K., and Weber, K. (1983) *J. Biol. Chem 258*, 365−369.

BI972192P